A Monte Carlo Simulation of the Electrochemical Reduction of Alkyl Halides in Water. On the Validity of Marcus' Relationship

Víctor Pérez, José M. Lluch,* and Juan Bertrán

Contribution from the Departament de Química, Universitat Autònoma de Barcelona, 08193 Bellaterra, Barcelona, Catalonia, Spain

Received January 28, 1994®

Abstract: Microscopical Monte Carlo simulations of the electrochemical reductions of methyl fluoride and methyl chloride in water to give methyl radical and the corresponding halide anion have been performed. These are intended to be realistic models of a dissociative electron transfer reaction, a special case of an innersphere electron transfer process. Assuming a classical frame, the diabatic free energy curves corresponding to the precursor and successor complexes, in function of the reaction coordinate ΔE defined as the difference between the diabatic energy hypersurfaces for each configuration of the system, have been built up. The results of the computer simulations suggest that, unlike the outersphere electron transfer reactions, the Marcus' relationship cannot be applied straightforwardly to the dissociative electron transfer reactions in solution, its validity depending on the features of the solute internal potential energy. The relation of this fact with the central limit theorem is discussed.

Introduction

The concept of free energy functions plays a central role in the study of the electron transfer reactions in solution. The importance of using free energy rather than potential energy was realized by Marcus a long time ago.[1-6] His seminal theory, based on a macroscopic solvent continuum model, was originally developed for outersphere electron transfer reactions, in which no chemical bonds are broken or formed. One of the most fundamental achievements of the Marcus' theory is the nowadays widely used quadratic driving force-activation free energy Marcus' relationship[1,2,5,7]

$$\Delta F^{\ddagger} = \frac{(\Delta F_0 + \alpha)^2}{4\alpha} \tag{1}$$

that relates the activation free energy $\Delta F^{\ddagger}$ with the reaction free energy ΔF_0 and the reorganization free energy α (that is, the free energy released when the system evolves from equilibrium configurations corresponding to reactants to those corresponding to products, while an electronic wave function, that can be directly related to products in a valence-bond structure sense, is maintained to describe the solute).

It is easily shown that eq 1 is fulfilled if there exists a unique one-dimensional reaction coordinate, against which the free energy functions associated to reactants and products are paraboli of equal curvature.[8,9] Because of the clear anharmonicity of the internal potential energy interactions that appear, highly anharmonic free energy curves could be expected. However, recent microscopical computer simulations[9-15] have reproduced quite well the quadratic shape of the free energy curves for several outersphere electron transfer reactions in solution, the Marcus' relationship being validated for this kind of reaction. Then a linear response behavior is said to be held. This is a consequence of the Gaussian character of the probability distribution of solvent configurations versus a suitable reaction coordinate, which leads to parabolic curves.[16,17]

The scenario is clearly different for the innersphere electron transfer reactions. On the basis of a Morse curve description of the solute internal potential energies and a dielectric continuum approximation for the solvent fluctuational reorganization, the separability between both degrees of freedom being assumed, Savéant[18] has recently devised a simple model for dissociative electron transfer reactions in polar solvents that leads to the Marcus' relationship. These are reactions in which the transfer of the electron and the breaking of a bond are concerted processes, this being a special kind of innersphere electron transfers. By contrast, Kim and Hynes[19] have found an important deviation from the Marcus' relationship in a theoretical study of the SN1 ionic dissociation in solution. Their theoretical formulation employs a two-state model consisting of a pure covalent state and a pure ionic state and interprets the ionic dissociation process in terms of an electron transfer process between these two valence bond states, in this way becoming an innersphere electron transfer reaction.

Furthermore, a Monte Carlo simulation study by us[20,21] has suggested the lack of applicability of Marcus' relationship for the electrochemical reduction of hydrogen fluoride to give a hydrogen atom and a fluoride anion in a dipolar solvent, a very simple model of a dissociative electron transfer reaction. An interesting finding was that if a Morse curve and its repulsive part are employed to describe the solute internal potential energies (as

---

® Abstract published in *Advance ACS Abstracts,* September 15, 1994.

[1] Marcus, R. A. *J. Chem. Phys.* **1956**, *24*, 966.

[2] Marcus, R. A. *J. Chem. Phys.* **1956**, *24*, 979.

[3] Marcus, R. A. *Annu. Rev. Phys. Chem.* **1964**, *15*, 155.

[4] Marcus, R. A. *J. Chem. Phys.* **1965**, *43*, 679.

[5] Marcus, R. A.; Sutin, N. *Biochim. Biophys. Acta* **1985**, *811*, 265.

[6] Marcus, R. A. *J. Phys. Chem.* **1986**, *90*, 3460.

[7] Sutin, N. *Acc. Chem. Res.* **1982**, *15*, 275.

[8] Churg, A. K.; Weiss, R. M.; Warshel, A.; Takano, T. *J. Phys. Chem.* **1983**, *87*, 1683.

[9] King, G. M.; Warshel, A. *J. Chem. Phys.* **1990**, *93*, 8682.

[10] Hwang, J. K.; Warshel, A. *J. Am. Chem. Soc.* **1987**, *109*, 715.

[11] Kuharski, R. A.; Bader, J. S.; Chandler, D.; Sprik, M.; Klein, M. L.; Impey, R. W. *J. Chem. Phys.* **1988**, *89*, 3248.

[12] Chandler, D.; Kuharski, R. A. *Faraday Discuss. Chem. Soc.* **1988**, *85*, 1.

[13] Zichi, D. A.; Ciccotti, G.; Hynes, J. T.; Ferrario, M. *J. Phys. Chem.* **1989**, *93*, 6261.

[14] Tachiya, M. *J. Phys. Chem.* **1989**, *93*, 7050.

[15] González-Lafont, A.; Lluch, J. M.; Oliva, A.; Bertrán, J. *J. Comput. Chem.* **1991**, *12*, 1165.

[16] Carter, E. A.; Hynes, J. T. *J. Phys. Chem.* **1989**, *93*, 2184.

[17] Borgis, D.; Hynes, J. T. *J. Chem. Phys.* **1991**, *94*, 3619.

[18] (a) Savéant, J. M. *J. Am. Chem. Soc.* **1987**, *109*, 6788. (b) Andrieux, C. P.; Le Gorande, A.; Savéant, J. M. *J. Am. Chem. Soc.* **1992**, *114*, 6892. (c) Savéant, J. M. *J. Am. Chem. Soc.* **1992**, *114*, 10595.

[19] Kim, H. J.; Hynes, J. T. *J. Am. Chem. Soc.* **1992**, *114*, 10508.

[20] Pérez, V.; Lluch, J. M.; Bertrán, J. *J. Comput. Chem.* **1992**, *13*, 1057.

[21] Pérez, V.; Lluch, J. M.; Bertrán, J. *J. Mol. Liq.* **1994**, in press.

0002-7863/94/1516-10117$04.50/0

suggested by Savéant[18a]) instead of the calculated *ab initio* potentials, the free energy functions do not deviate markedly from the parabolic shape, the Marcus' relationship working well in this very special case.

To test the validity of Marcus' relationship for a special kind of innersphere electron transfers, in this paper we have performed a microscopical Monte Carlo simulation of the electrochemical reduction of alkyl halides in a polar solvent to give alkyl radicals and halide anions, a realistic dissociative electron transfer reaction. To this end we have chosen methyl fluoride and methyl chloride as the simplest examples of alkyl halides that allow us to study the cleavage of a carbon–halogen σ-bond concerted with the electron transfer. Water has been taken as example of a polar solvent.

Methodology

To describe the electron transfer we will employ a diabatic two-state model consisting of the methyl halide surrounded by the solvent plus an electron inside an electrode (precursor complex), and the methyl halide anion immersed in the solvent, once the electron has already shifted from the electrode (successor complex).[22,23] Assuming a classical frame,[4,24,25] the radiationless electron transfer must take place at the S^* intersection region of the diabatic potential energy hypersurfaces corresponding, respectively, to the precursor complex (H_{pp}) and the successor complex (H_{ss}). Random thermal fluctuations in the nuclear configurations of the precursor complex, involving the nuclear coordinates of both the solute and the solvent, occur until this S^* region is reached, then the energies of both diabatic states becoming equal and the electron jump happening. The appearance of the proper fluctuations costs free energy. It is this free energy that determines the rate of the reaction and whose analysis is the object of this work. The electronic coupling integral between both diabatic states is supposed to be large enough for the reactants to be converted into products with unit probability in the intersection region but small enough to be neglected in calculating the amount of internal energy required to reach S^*.

In this paper the energies of the H_{pp} and H_{ss} diabatic hypersurfaces have been obtained by adding three kinds of pairwise additive potential functions: the solute internal potential energy, the solvent–solvent interaction, and the solute–solvent interaction. Thermal fluctuations have been generated by means of the Monte Carlo method. Both the pair potentials and the statistical simulation strategy are discussed below.

Solute Internal Potential Energy. This is the potential corresponding to the gas phase reaction. In the absence of the solvent, the precursor complex consists of the methyl halide plus an electron inside an electrode. Its energy is calculated as the sum of the methyl halide energy and a constant value that represents the Fermi level energy of the electrode. Note that the solution exchanges electrons with the metal at the Fermi level because these are the most energetic electrons for reduction. On the other hand, the successor complex in gas phase is considered to be the methyl halide anion in the electronic state that leads to the diabatic dissociation in halide anion and methyl radical.

In order to build up the gas phase diabatic pair potentials, a set of *ab initio* calculations has been carried out with the GAMESS[26] program for several values of the C–X interatomic distance for the methyl halides and the methyl halide anions. First of all, the energy at each C–X distance, the rest of geometrical parameters being optimized, has been obtained with the restricted open Hartree–Fock formalism. After several trials, the 6-31G** basis set has been finally chosen to describe all the atoms, the fluorine and chlorine atoms being supplemented by the diffuse sp shell that is employed in the 6-31+G** for these halogen atoms. This atypical basis set allows us to refer to the obtained curves as diabatic, in the sense that the nature of the occupied molecular orbitals is maintained during the dissociation process. So, for the anionic species, the additional electron occupies a σ^* C–X antibonding molecular orbital along the dissociation, this molecular orbital becoming a carbon $2p_z$ atomic orbital when the methyl halide anion is completely broken. Conversely, the whole 6-31+G** basis set localizes the additional electron on a σ nonbonding molecular orbital practically centered on the carbon atom at short C–X distances, while at larger C–X distances, after the corresponding crossing, the electron occupies the σ^* C–X antibonding molecular orbital, an adiabatic rather than a diabatic dissociation being done. It has to be mentioned at this point that the problem associated with the inclusion of diffuse functions in the basis set to obtain a reliable description of the anions and their diabatic dissociation has been recently discussed by several authors.[27–34]

Table 1. CH_3F and CH_3Cl: Characteristics of the Neutral Molecule in Gas Phase

	CH_3F		CH_3Cl	
	exp	this work	exp	this work
d_{C-X}[(a)]	1.38[(e)]	1.37	1.78[(i)]	1.79
VEA[(b)]	143.0[(f)]	141.8	79.5[(f)]	68.2
D_e[(c)]	108.0[(g)]	105.6	83.4[(i)]	80.4
EA of X[(d)]	79.6[(h)]	63.9	83.4[(i)]	77.6

[(a)] Ground-state C–X distance in Å. [(b)] Vertical electron affinity in kcal/mol. [(c)] C–X bond dissociation energy in kcal/mol. [(d)] Electron affinity of X in kcal/mol. [(e)] From ref 38. [(f)] From ref 33. [(g)] From ref 39. [(h)] From ref 40. [(i)] From ref 41.

From the optimized structures along the C–X coordinate, using our 6-31G** augmented basis set, the energies have been recalculated by means of a truncated configuration interaction (CI) expansion[35–37] that includes single, double, triple, and quadruple excitations (CISDTQ). The CI space involves 42 301, 35 916, 24 921, and 62 760 spin-adapted configurations for the methyl fluoride, methyl fluoride anion, methyl chloride, and methyl chloride anion, respectively. For the anionic species CI calculations have been performed from the corresponding ROHF optimized molecular orbitals. However, in order to obtain a best description of the wave function, the CI calculations of the neutral molecules have been done from the ROHF optimized molecular orbitals corresponding to their associated anions but using the geometrical structure of the neutral species.

From the *ab initio* calculations, energy profiles with a minimum and with a repulsive shape arise, respectively, for the dissociation of the C–X bond in the methyl halides and the methyl halide anions. To test the goodness of the results, in Table 1 we have displayed different experimental values along with our cor-

---

(22) Newton, M. D.; Sutin, N. *Annu. Rev. Phys. Chem.* **1984**, *35*, 437.

(23) Newton, M. D. *Int. J. Quantum Chem., Quantum Chem. Symp.* **1980**, *14*, 363.

(24) Sutin, N. *Annu. Rev. Nucl. Sci.* **1962**, *12*, 285.

(25) Hush, N. S. *Trans. Faraday Soc.* **1965**, *57*, 155.

(26) Schmidt, M. W.; Baldridge, K. K.; Boatz, J. A.; Jensen, J. H.; Koseki, S.; Gordon, M. S.; Nguyen, K. A.; Windus, T. L.; Elbert, S. T. *GAMESS Q.C.P.E. Bull.* **1990**, *10*, 52.

(27) Hottoka, M.; Roos, B. O.; Eberson, L. *J. Chem. Soc., Perkin Trans. II* **1986**, 1979.

(28) Benassi, R.; Bernardi, F.; Bottoni, A.; Robb, M. A.; Taddei, F. *Chem. Phys. Lett.* **1989**, *161*, 79.

(29) Guerra, M. *Chem. Phys. Lett.* **1990**, *167*, 315.

(30) Falcetta, M.; Jordan, K. D. *J. Phys. Chem.* **1990**, *94*, 5666.

(31) Bertrán, J.; Gallardo, I.; Moreno, M.; Savéant, J. M. *J. Am. Chem. Soc.* **1992**, *114*, 9576.

(32) Guerra, M.; Jones, D.; Distefano, G.; Scagnolari, F.; Modelli, A. *J. Chem. Phys.* **1991**, *94*, 484.

(33) Modelli, A.; Scagnolari, F.; Distefano, G.; Jones, D.; Guerra, M. *J. Chem. Phys.* **1992**, *96*, 1061.

(34) Pérez, V.; Lluch, J. M.; Bertrán, J. *J. Mol. Struct. Theochem.* **1992**, *254*, 51.

(35) Pople, J. A.; Binkley, J. S.; Seeger, R. *Int. J. Quantum Chem., Quantum Chem. Symp.* **1976**, *10*, 1.

(36) Pople, J. A.; Seeger, R.; Krishann, R. *Int. J. Quantum Chem., Quantum Chem. Symp.* **1977**, *11*, 149.

(37) Pople, J. A.; Seeger, R.; Krishann, R. *Int. J. Quantum Chem., Quantum Chem. Symp.* **1977**, *11*, 164.

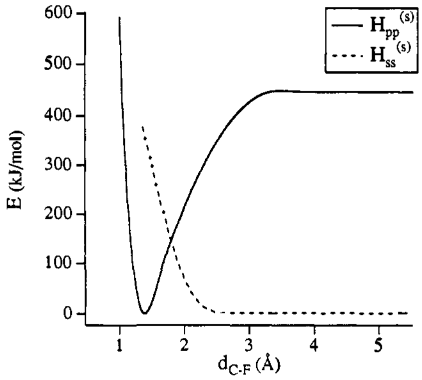

Figure 1. Fitted cubic spline curves representing the solute internal potential energy in respect of the d_{C-F} distance, for the precursor (solid line) and the successor (dotted line) complexes, corresponding to the reduction of methyl fluoride in gas phase.

responding theoretical ones. From the first to fourth row, the C–X internuclear distance corresponding to the equilibrium structure of methyl halides (d_{C-X}), the vertical electron affinity (VEA), the dissociation energy (D_0), and the halogen atom's electron affinity are shown successively. It can be seen that a good agreement with the experimental values exists, what warrants the validity of the gas phase pair potential built up in this work. It can be underlined that reliable theoretical values of VEA are not easy to obtain.

Finally, the *ab initio* results have been employed to obtain analytic functions to describe the solute internal potential energy of the precursor and the successor complexes versus d_{C-X}. As mentioned below, in order to perform the statistical simulations, the methyl group will be modeled as a single unit centered on the carbon atom,[42] in such a way that the d_{C-X} parameter is enough to specify the solute geometry. Cubic spline fittings have been used to determine those analytic functions.

The Fermi level energy has been chosen as the value that makes the reaction energy equal to zero in the gas phase. This implies an energy for the electron inside the metal of 174.9 and 11.7 kJ/mol for the precursor complexes containing the methyl fluoride and the methyl chloride, respectively. The fitted cubic spline curves representing the solute internal potential energy for the precursor and successor complexes corresponding to the reduction of the methyl fluoride in gas phase are shown in the Figure 1.

Water–Water and Solute–Water Pair Potentials. For the water–water interactions the well-known TIP4P potential, developed by Jorgensen *et al.*,[43,44] has been adopted. This potential involves four interaction centers.

On the other hand, the interactions water–solute are described by means of an analytical function V_{W-S} containing coulombic interactions between all intermolecular pairs of charges along with Lennard–Jones terms r^{-6} and r^{-12} between all intermolecular pairs of atoms. It has been recalled that the methyl group is represented by a single unit

$$V_{W-S} = \sum_{i}^{S} \sum_{j}^{W} \left(\frac{q_i q_j}{r_{ij}} + \frac{C_i C_j}{r_{ij}^{12}} - \frac{B_i B_j}{r_{ij}^{6}} \right) \qquad (2)$$

where *i* and *j* indexes stand for the solute and water interaction centers, respectively. The *B* and *C* parameters of all interaction centers along with the charges associated with the water interaction centers have been taken from several intermolecular potentials developed by the Jorgensen's group.[43–46] Regarding the solute charges, it has to be noted that they vary as the reaction proceeds. For this reason, we have used the Mulliken charges obtained using the 6-31G** augmented basis set for several d_{C-X} distances, to fit analytical functions that give the q_i values in front of the d_{C-X} distances to be introduced in eq 2. To test the goodness of the water–solute interaction potential functions, for instance, we have found the minimum energy structure corresponding to the CH_3F–H_2O complex. From our pair potential function the interaction energy and the fluorine–oxygen distance are, respectively, –5.02 kcal/mol and 2.75 Å. An *ab initio* calculation using the 6-31G** augmented basis set with a CI expansion including single and double excitations gives the values of –5.07 kcal/mol and 2.92 Å, respectively. The good agreement between both sets of values shows the validity of the fitted water–solute pair potentials.

Statistical Simulation Strategy. We have studied the dissociative electron transfer reactions by simulating the precursor complex and the successor complex in a solution containing 200 water molecules at $T = 298$ K. In the simulations the halogen atom is held fixed, and the methyl group as well as the water molecules were moved to generate configurations using the Monte Carlo method[47,48] within the Metropolis algorithm.[49] The size of the box has been chosen in such a way that 200 water molecules would give a density of about 1 g/cm³. Periodic boundary conditions under the minimum image convention have been employed. For all simulations a preliminary equilibration of the system followed by statistical analysis performed on additional configurations has been carried out. These simulations were run using a program written by us.

For each generated configuration the value $\Delta E = H_{ss} - H_{pp}$ has been calculated. This parameter has been shown to behave as a good reaction coordinate for the diabatic free energy curves in electron transfer reactions.[8,13,14,16,50,51] The configuration space was partitioned in different subsets S, each one being associated with a particular value ΔE_s of the reaction coordinate ΔE. For practical purposes, the criterion $|\Delta E - \Delta E_S| \leq 5$ kJ/mol has been adopted in order to classify a given configuration as belonging to a subset S. We have identified the reactants' region (S_R) with the most populated interval when the H_{pp} potential is used. Conversely, the products' region (S_P) is the most populated interval corresponding to the H_{ss} potential. The intersection region S* corresponds to the interval centered at the value of $\Delta E_S = 0$ kJ/mol. Therefore, this value of the reaction coordinate explicitly characterizes the transition structures for the electron transfer. The activation free energy $\Delta F^{\ddagger}$ corresponds to the transition from S_R to S*, in such a way that the factor $\exp(-\Delta F^{*}/kT)$ expresses the probability that the reaction system will be in the transition state region S* relative to the probability of being in S_R.

Due to the high value of ΔF^{*} for our reactions, the complete sampling of the configuration space in order to obtain the diabatic free energy curves as a function of ΔE_S would require an extremely long simulation. To circumvent this problem we have used a strategy previously developed by Warshel *et al.*[9,10,52] A mapping potential energy hypersurface of the form $H_m = (1 - \lambda_m)H_{pp} + \lambda_m H_m$ is defined, H_{pp} and H_{ss} being calculated from the potential

---

(38) Clark, W. W.; DeLucia, F. C. *J. Mol. Struct.* **1976**, *32*, 29.

(39) Kerr, J. A. *Chem. Rev.* **1966**, *66*, 465.

(40) Berry, R. S.; Rice, S. A.; Ross, J. *Physical Chemistry*; Wiley: New York, 1980; p 574.

(41) Weissman, M.; Benson, S. W. *J. Phys. Chem.* **1983**, *87*, 243.

(42) Jorgensen, W. J. *J. Am. Chem. Soc.* **1981**, *103*, 341.

(43) Jorgensen, W. J. *J. Am. Chem. Soc.* **1981**, *103*, 335.

(44) Jorgensen, W. J.; Chandrasekhar, J.; Madura, J. D.; Impey, R. W.; Klein, M. L. *J. Chem. Phys.* **1983**, *79*, 926.

(45) Cournoyer, M. E.; Jorgensen, W. J. *Mol. Phys.* **1984**, *51*, 119.

(46) Chandrasekhar, J.; Smith, S. F.; Jorgensen, W. L. *J. Am. Chem. Soc.* **1985**, *107*, 154.

(47) Wood, W. W. *Fundamental Problems in Statistical Mechanics III*; Cohen, E. G. D., Ed.; North-Holland: Amsterdam, 1975; pp 331–388.

(48) Valleau, J. P.; Whittington, S. G. *Statistical Mechanics. Part A: Equilibrium Techniques*; Berne, B. J., Ed.; Plenum Press: New York, 1977; pp 137–168.

(49) Metropolis, N.; Rosenbluth, A. W.; Rosenbluth, M. N.; Teller, A. H.; Teller, E. *J. Chem. Phys.* **1953**, *21*, 1087.

(50) Warshel, A. *J. Phys. Chem.* **1982**, *86*, 2218.

(51) Yoshimori, A.; Kakitani, T.; Enomoto, Y.; Mataga, N. *J. Phys. Chem.* **1989**, *93*, 8316.

functions obtained above. The parameter λ_m changes from 0 to 1 on movement from the precursor to the successor states. With the H_m potential corresponding to $\lambda_m = 0$ the most populated subspace is S_R. As λ_m increases, the system is forced to evolve toward the intersection reaction S^*. With the H_m potential corresponding to $\lambda_m = 1$ the most populated subspace is S_P. Now the diabatic free energies corresponding to the precursor and the successor complexes along the reaction coordinate are obtained by using the expressions[9,10,15,52] as a function of ΔE_S:

$$\Delta F_{pp}(\Delta E_S) = \Delta F_{0\to m} - \lambda_m \Delta E_S - kT \ln\left[\frac{q_m^{(S)}}{Q_m}\frac{Q_{pp}}{q_{pp}^{(S_R)}}\right] \quad (3)$$

$$\Delta F_{ss}(\Delta E_S) = \Delta F_{1\to m} + (1-\lambda_m)\Delta E_S - kT \ln\left[\frac{q_m^{(S)}}{Q_m}\frac{Q_{ss}}{q_{ss}^{(S_P)}}\right] \quad (4)$$

The last term of eqs 3 and 4 involves ratios of partition functions. So, the factor $q_m^{(S)}/Q_m$ is the probability that, using the H_m potential, the configurations generated belongs to the subset S. The ratio $q_{pp}^{(S_R)}/Q_{pp}$ in eq 3 represents the probability that, using the H_{pp} diabatic potential, the configurations generated belong to the reactants' subset S_R. Analogously, the factor $q_{ss}^{(S_P)}/Q_{ss}$ in eq 4 represents the probability that, using the H_{ss} diabatic potential, the configurations generated belong to the products' subset S_P.

The values $\Delta F_{0\to m}$ and $\Delta F_{1\to m}$ have been calculated by using statistical perturbation theory. This approach follows from eq 5 which expresses the free energy difference between systems with mapping potentials $H_{j'}$ and H_j by

$$\Delta F(\lambda_j \to \lambda_{j'}) = -kT \ln\left\langle \exp\frac{-(H_{j'} - H_j)}{kT}\right\rangle_{H_j} \quad (5)$$

The average is for sampling based on the potential H_j, so the $H_{j'}$ potential corresponds to a perturbed system. Therefore

$$\Delta F_{0\to m} = \Delta F(\lambda_0 = 0 \to \lambda_m) = \sum_{j=0}^{m-1} \Delta F(\lambda_j \to \lambda_{j+1}) \quad (6)$$

To transform the potential smoothly and to avoid large perturbations, λ_j has been increased in small steps from 0 to 1. Simulations have been run in both directions, $\lambda_j \to \lambda_{j+1}$ and $\lambda_{j+1} \to \lambda_j$, except at the two end points. This is known as double-ended sampling. It is facilitated by using double-wide sampling.[53] Specifically, the free energy differences for $\lambda_j \to \lambda_{j+1}$ and $\lambda_j \to \lambda_{j-1}$ can be obtained simultaneously, since both require sampling based on the λ_j system. To evaluate numerically $\Delta F(\Delta E_S)$ with eqs 3 and 4, we have used in each case the mapping potential H_m for which the most populated subset S is the one centered at ΔE_S. Following this procedure, each calculation converges very fast.

To test the validity of the Marcus' relationship ΔF_0 and α values are obtained from the Monte Carlo simulations through the equations

$$\Delta F_0 = \Delta F_{pp}(0) - \Delta F_{ss}(0) \quad (7)$$

$$\alpha = \Delta F_{ss}(\Delta E_S^{S_R}) - \Delta F_{ss}(\Delta E_S^{S_P}) \quad (8)$$

where $\Delta E_S^{S_R}$ and $\Delta E_S^{S_P}$ are the values of the reaction coordinate associated with the reactants' region (S_R) and the products' region (S_P), respectively.

Table 2. Values of the Most Probable Carbon–Fluorine Interatomic Distance (d_{C-F}) for Each Mapping Potential (Associated with the λ_m Value) in the FHDE Simulation, along with the Percentage of Configurations That Presents This d_{C-F} Value

λ_m	d_{C-F} (Å)	% configrtns	λ_m	d_{C-F} (Å)	% configrtns
0.000	1.390	17.920	0.500	2.130	5.610
0.050	1.400	16.000	0.550	2.210	5.680
0.100	1.410	15.200	0.600	2.260	5.480
0.150	1.410	14.260	0.650	2.330	5.450
0.200	1.430	13.490	0.700	2.380	5.080
0.250	1.460	12.440	0.750	2.440	4.680
0.300	1.460	10.150	0.800	2.510	4.960
0.350	1.500	6.330	0.850	2.590	4.260
0.360	1.540	4.750	0.900	2.670	1.800
0.375	1.940	2.540	0.950	4.900	1.440
0.400	1.960	4.590	1.000	5.470	0.960
0.450	2.050	4.710			

Results and Discussion

First of all we will present the results of the simulation corresponding to the electrochemical reduction of the methyl fluoride, which from here on will be called fluoride-high-dissociation-energy (FHDE) simulation. In all, a total of 92 460 000 configurations have been generated, being distributed in 23 runs. Each run consisted of an equilibrium phase of 2 010 000 configurations followed by averaging over 2 010 000 additional configurations.

As λ_m moves from 0 to 1 the system is forced to evolve from reactants to products. The most probable carbon–fluorine interatomic distances (d_{C-F}) for each mapping potential, along with the percentage of configurations that presents this d_{C-F} value, are displayed in Table 2. At $\lambda_m = 0$ (precursor complex) the most likely distance is 1.39 Å (a value slightly longer than the one corresponding to the methyl fluoride equilibrium distance in the gas phase[38]), an important percentage of configurations appearing with this value. As λ_m increases (going to products), d_{C-F} progressively augments, leading to the breakage of the C–F bond for $\lambda_m = 1$. In addition, the spread of distances becomes broader. Both facts are a consequence of the increasing weight of the H_{ss} diabatic potential whose solute internal potential energy component is dissociative and quite flat at long C–F distances.

In Table 3 the computed free energy differences $\Delta F(\lambda_j \to \lambda_{j'})$ defined by eq 5 are displayed. Although there is no significant hysteresis, the accumulated free energy values $\Delta F_{0\to m}$, shown in Table 4, have been obtained by averaging the results of the two paths in opposite directions, this way the errors tending to be cancelled out. The data exhibited in Table 4, along with the eqs 3 and 4, and taking into account the expression

$$\Delta F_{1\to m} = \Delta F_{0\to m} - \Delta F_{0\to 1} \quad (9)$$

lead to the diabatic free energy values along the reaction coordinate, which have been represented by squares in Figure 2. As λ_m increases, the most populated subspace evolves from being centered around $\Delta E_S = 409.5$ kJ/mol (subspace S_R, corresponding to reactants) to being centered around $\Delta E_S = -1460.5$ kJ/mol (subspace S_P, corresponding to products). Although the determination of the exact value of λ_m for which S^* is the most populated subspace is very subtle, the results indicate that it has to be within the interval $\lambda_m = 0.35$–0.375.

From the diabatic free energy values we have tried to obtain a quadratic least-squares fitting of ΔF_{pp} and ΔF_{ss} versus ΔE_S. Two parabolic curves (represented in Figure 2) have been generated, both functions having the same curvature. However, the minima corresponding to these fitted diabatic free energy curves appear at $\Delta E_S = 588.9$ and $\Delta E_S = -1434.5$ kJ/mol, respectively, for the precursor and successor complexes. These

---

(52) Hwang, J. K.; King, G.; Creighton, S.; Warshel, A. *J. Am. Chem. Soc.* **1988**, *110*, 5297.

(53) Jorgensen, W. L.; Ravimohan, C. J. *J. Chem. Phys.* **1985**, *83*, 3050.

Table 3. Computed Free Energy Differences (in kJ/mol) Obtained in the FHDE Simulation for the Transformation from the Unperturbed to the Perturbed System

		ΔF	
λ_j	λ_{j+1}	$j \rightarrow j+1$	$j+1 \rightarrow j$
0.000	0.050	20.155	−18.724
0.050	0.100	17.093	−16.953
0.100	0.150	15.224	−14.978
0.150	0.200	13.464	−13.914
0.200	0.250	12.194	−11.592
0.250	0.300	8.956	−9.756
0.300	0.350	5.887	−6.238
0.350	0.360	−0.893	0.024
0.360	0.375	−1.572	1.203
0.375	0.400	−6.132	6.649
0.400	0.450	−20.353	20.103
0.450	0.500	−25.830	27.145
0.500	0.550	−30.311	30.814
0.550	0.600	−33.237	34.469
0.600	0.650	−36.978	35.516
0.650	0.700	−38.270	38.941
0.700	0.750	−41.587	42.125
0.750	0.800	−44.817	45.820
0.800	0.850	−48.895	46.673
0.850	0.900	−50.017	54.184
0.900	0.950	−65.390	68.958
0.950	1.000	−70.953	72.014

Table 4. FHDE Simulation: Accumulated Free Energy (in kJ/mol), ΔE_S (in kJ/mol) for the Most Populated Subset S When Each Mapping Potential H_m, Associated with λ_m, Is Used, and Ratios of Partition Functions

λ_m	$\Delta F_{0\rightarrow m}$	ΔE_S	$q_m^{(S)}/Q_m$
0.000	0.000	409.500	0.107
0.050	19.440	349.500	0.097
0.100	36.463	319.500	0.098
0.150	51.565	299.500	0.103
0.200	65.254	269.500	0.098
0.250	77.147	199.500	0.082
0.300	86.504	169.500	0.072
0.350	92.567	79.500	0.039
0.360	92.108	49.500	0.037
0.375	90.720	−310.500	0.025
0.400	84.329	−350.500	0.058
0.450	64.100	−480.500	0.055
0.500	37.612	−590.500	0.075
0.550	7.050	−640.500	0.079
0.600	−26.803	−720.500	0.082
0.650	−63.050	−740.500	0.078
0.700	−101.655	−790.500	0.075
0.750	−143.512	−880.500	0.077
0.800	−188.831	−940.500	0.074
0.850	−236.616	−980.500	0.072
0.900	−288.717	−1310.500	0.042
0.950	−355.896	−1400.500	0.090
1.000	−427.380	−1460.500	0.093

values are far from the above mentioned true values coming directly from the Monte Carlo simulation (409.5 and −1460.5 kJ/mol). In other words, neither ΔF_{pp} nor ΔF_{ss} can be adjusted to parabolas with minima appearing in the regions associated to reactants and products, respectively. As a consequence, a clear deviation of the Marcus' relationship can be expected. In effect, if the values $\Delta F_0 = -427.0$ kJ/mol and $\alpha = 836.6$ kJ/mol arising from the numerical simulation are taken to be introduced in the Marcus' relationship (1), a free energy barrier relative to the reactant region of $\Delta F_M{}^{\ddagger} = 50.11$ kJ/mol is obtained. This value differs clearly from the true value $\Delta F^{\ddagger} = 78.2$ kJ/mol emerging from the simulation, a relative error as large as 36% being involved.

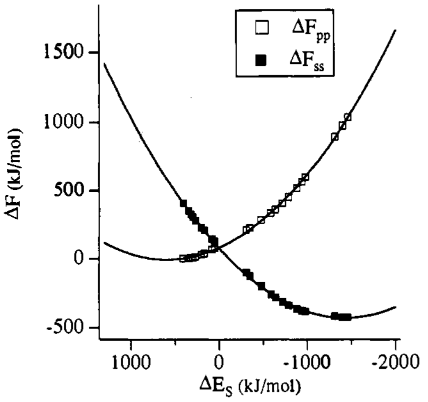

Figure 2. Diabatic free energy curves for the precursor (white squares) and the successor (black squares) complexes in respect of values ΔE_S of the reaction coordinate ΔE, corresponding to the FHDE simulation.

Table 5. CH_3Cl Simulation: Accumulated Free Energy (in kJ/mol), ΔE_S (in kJ/mol) for the Most Populated Subset S When Each Mapping Potential H_m, Associated with λ_m, Is Used, and Ratios of Partition Functions

λ_m	$\Delta F_{0\rightarrow m}$	ΔE_S	$q_m^{(S)}/Q_m$
0.000	0.000	329.500	0.109
0.050	15.883	309.500	0.103
0.100	30.418	269.500	0.114
0.150	43.539	249.500	0.111
0.200	54.970	209.500	0.107
0.250	64.928	179.500	0.098
0.300	74.265	199.500	0.073
0.350	80.935	89.500	0.090
0.400	84.695	59.500	0.078
0.450	85.138	−0.500	0.057
0.500	73.524	−310.500	0.069
0.550	55.165	−410.500	0.062
0.600	33.513	−480.500	0.070
0.650	8.300	−530.500	0.081
0.700	−20.029	−590.500	0.076
0.750	−50.447	−610.500	0.077
0.800	−85.786	−820.500	0.103
0.850	−127.492	−860.500	0.106
0.900	−171.835	−910.500	0.119
0.950	−217.916	−920.500	0.093
1.000	−265.790	−980.500	0.105

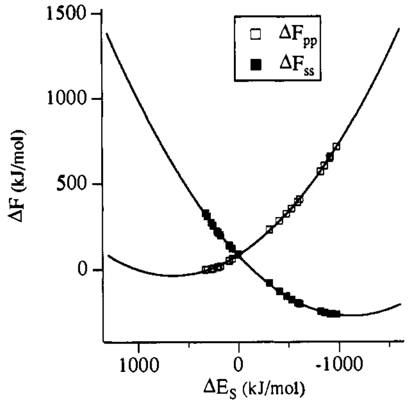

Figure 3. Diabatic free energy curves for the precursor (white squares) and the successor (black squares) complexes in respect of values ΔE_S of the reaction coordinate ΔE, corresponding to the reduction of methyl chloride in solution.

As for the electrochemical reduction of the methyl chloride, a total of 84 420 000 configurations have been generated, being divided in 21 runs, each one consisting of 2 010 000 configurations for equilibration and 2 010 000 additional configurations of averaging. From the data collected in Table 5, the diabatic free energy values along the reaction coordinate, which are shown by squares in Figure 3, have been obtained. Quadratic fittings of ΔF_{pp} and ΔF_{ss} have also been attempted here. Again the minima associated to the fitted diabatic free energy parabolic functions corresponding to the precursor and successor complexes appear very far (at $\Delta E_S = 649.4$ and $\Delta E_S = -1126.8$ kJ/mol, respectively) from the true values coming directly from the simulation (at ΔE_S

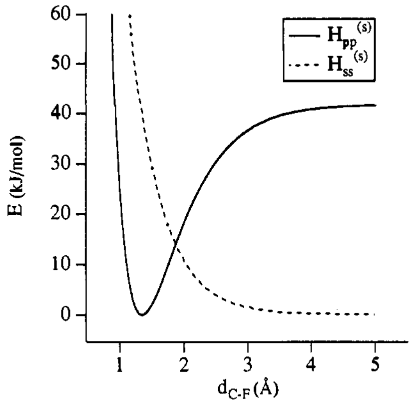

Figure 4. Gas phase diabatic energy curves for the precursor (solid line) and the successor (dotted line) complexes, corresponding to the FLDE simulation.

= 329.5 and ΔE_S = −980.5 kJ/mol for the reactant's region and the products' region, respectively), then the quadratic adjustment becoming unreasonable. As a matter of fact, the values ΔF_0 = −265.7 and α = 595.2 kJ/mol resulting from the simulation lead through Marcus' relationship to a free energy barrier $\Delta F_M^{\ddagger}$ = 45.6 kJ/mol that involves a relative error as large as 44% when compared with the true value arising from the simulation ($\Delta F^{\ddagger}$ = 82.2 kJ/mol).

Up to this point it seems our Monte Carlo simulations suggest that Marcus' relationship does not hold for the electrochemical reduction of methyl fluoride and methyl chloride in water, this result being in disagreement with the computer simulations for outersphere electron transfer reactions.[9-15] Actually, the practical difference between both kind of microscopical simulations rises from the solute internal potential energy that is employed to describe the breaking of the corresponding bond. This term exists for dissociative electron transfer simulations but is absent in the outersphere electron transfer ones. Indeed it has to play an important role in the process, since, for instance, the gas phase potential we have used to represent the precursor complex for the methyl fluoride case implies a dissociation energy as large as 441.8 kJ/mol, the bond to be broken being strong enough to completely modify the scenario corresponding to the outersphere situation. Then, in what follows we have investigated if the fulfilment of the Marcus' relationship depends on the size of this dissociation energy. To this aim, we have repeated twice the Monte Carlo simulation corresponding to the electrochemical reduction of the methyl fluoride, maintaining the same solute–water and water–water pair potentials used for the FHDE simulation but altering the solute internal potential energy in such a way that the dissociation energy is clearly reduced. The new analytical functions to describe the gas phase diabatic pair potentials lead to the same shape, d_{C-F} gas phase equilibrium internuclear distance of the methyl fluoride (1.37 Å), and d_{C-F} gas phase diabatic crossing value (1.81 Å) as corresponding to the true ab initio gas phase pair potentials employed in the FHDE simulations, although involving a different value for the methyl fluoride dissociation energy. When this dissociation energy has been chosen to be 83.7 or 41.8 kJ/mol, the corresponding Monte Carlo simulations have been called fluoride-medium-dissociation-energy (FMDE) or fluoride-low-dissociation-energy simulations (FLDE), respectively. The gas phase diabatic energy profiles corresponding to this last case have been drawn in Figure 4. For each one of these simulations a total of 84 420 000 configurations, divided in 21 runs, have been generated. Although neither the FMDE nor the FLDE simulation represents any definite chemical system, both are useful to isolate the relevant importance of the solute pair potentials.

Table 6. Reaction Energy, Reorganization Energy, Energy Barrier Obtained by Means of the Marcus' Relationship, True Energy Barrier Obtained in Our Calculations, and Relative Error Introduced by the Marcus' Relationship, for Each Simulation in Gas Phase

simulation	ΔE_0[a]	α_g[a]	$\Delta E_M^{\ddagger}$ [a]	$\Delta E^{\ddagger}$ [a]	% error
HF	0.0	168.9	42.2	94.5	55
HF(Morse)	0.0	565.3	141.3	141.3	0
CH_3F(FHDE)	0.0	376.8	94.2	145.4	35
CH_3F(FMDE)	0.0	78.5	19.6	28.1	30
CH_3F(FLDE)	0.0	39.2	9.8	14.0	30
CH_3Cl	0.0	273.7	68.4	125.1	45

(a) In kJ/mol.

Table 7. Reaction Free Energy, Reorganization Free Energy, Free Energy Barrier Obtained by Means of the Marcus' Relationship, True Free Energy Barrier Obtained in our Calculations, and Relative Error Introduced by the Marcus' Relationship, for Each Electrochemical Reduction Simulation in Solution

simulation	ΔF_0[a]	α[a]	$\Delta F_M^{\ddagger}$ [a]	$\Delta F^{\ddagger}$ [a]	% error
HF	−126.3	305.9	26.3	74.0	64
HF(Morse)	−99.5	702.5	129.4	135.2	4
CH_3F(FHDE)	−427.0	836.6	50.1	78.2	36
CH_3F(FMDE)	−432.7	541.5	6.1	5.5	11
CH_3F(FLDE)	−439.0	509.9	2.1	2.3	9
CH_3Cl	−265.7	595.2	45.6	82.2	44

(a) In kJ/mol.

For brevity we will omit here the details regarding the obtained diabatic free energy values along the reaction coordinate and the corresponding attempts to achieve quadratic fittings and will directly proceed to assess the applicability of the Marcus' relationship. For the sake of comparison we present the results corresponding to the FMDE and FLDE simulations, along with the ones coming from the FHDE and methyl chloride simulations. In addition, the results obtained previously for the electrochemical reduction of hydrogen fluoride[20] with ab initio gas phase diabatic pair potentials[20,34] (HF simulation) and for the same system when a Morse curve[21] and its repulsive part are used to represent the gas phase diabatic pair potentials associated, respectively, to the precursor and successor complexes (HF More simulation), have been included as well. In Table 6 we have collected the reaction energy, the reorganization energy, the energy barrier relative to the reactant which is obtained by introducing these two values in the Marcus' relationship, the energy barrier arising directly from the crossing point between both gas phase diabatic pair potentials, and the relative error introduced by the Marcus' relationship, for each simulation in gas phase. That is, all those values are found just considering the gas phase diabatic pair potentials. Because only a coordinate (the one associated to the bond that has to be broken) is explicitly involved in our gas phase calculations, it has to be noted that the energy values are equivalent to free energy values. On the other hand, in Table 7 we have assembled the reaction free energy, the reorganization free energy, the free energy barrier relative to the reactant's region which is obtained by introducing these two values in the Marcus' relationship, the free energy barrier directly stemming from the Monte Carlo simulation, and the relative error introduced by the Marcus' relationship, for each electrochemical reduction simulation in solution.

A detailed analysis of both tables reveals several interesting points. First of all, in gas phase only the HF Morse case fulfills the Marcus' relationship. This is due to the fact that all the gas phase diabatic pair potentials (remember that in our gas phase results energy and free energy are equivalent) are highly anharmonic. However, if the coordinate $Q = \exp(-\beta y)$ is defined, both the Morse curve and its repulsive part are quadratic functions of Q with the same curvature, then the Marcus' relationship is exact.[21,54] For the HF Morse simulation Marcus' relationship works well even in solution (only a very small relative error, that could be attributed to numerical errors, appears). As a matter

---

(54) Marcus, R. A. *J. Phys. Chem.* **1992**, *96*, 1753.

of fact, it is clear that if Marcus' relationship runs well for outersphere electron transfer reactions, the addition of quadratic contributions of the solute does not modify its validity. On the other hand, the remaining five simulations can be classified into two different groups. For three of them the relative error in solution is roughly as large as in gas phase. Conversely, for both the FMDE and FLDE simulations (those that would involve a C–F bond relatively easy to break in gas phase) the Marcus' relationship behaves well enough in solution, despite its clear failure in gas phase.

The central limit theorem could be the origin of the intriguing results above.[55] Roughly speaking, this theorem states that, under a variety of conditions, the distribution of sums of random variables tends to a normal distribution as the number of random variables tends to infinity. One set of conditions guaranteeing this limiting distribution is independence of the random variables and identical distributions with finite variances, but other conditions are also available that do not require identical distributions or even independence. If the distributions are not identical, what is required is that each random variable has a small contribution to the total value of the sum.

Now we will examine our results under the light of the central limit theorem. Let us focus on the distribution of the reaction coordinate ΔE. Assuming that the diabatic energy hypersurfaces can be calculated as addition of three kinds of pairwise additive potential functions, they can be written as

$$H_{\mathrm{pp}} = H_{\mathrm{pp}}^{(\mathrm{s})} + \sum_{\mathrm{i}} H_{\mathrm{pp,i}}^{(\mathrm{s-w})} + \sum_{\mathrm{i}}\sum_{\mathrm{j>i}} \mathrm{H}_{\mathrm{pp,ij}}^{(\mathrm{w})} \qquad (10)$$

and

$$H_{\mathrm{ss}} = H_{\mathrm{ss}}^{(\mathrm{s})} + \sum_{\mathrm{i}} H_{\mathrm{ss,i}}^{(\mathrm{s-w})} + \sum_{\mathrm{i}}\sum_{\mathrm{j>i}} \mathrm{H}_{\mathrm{ss,ij}}^{(\mathrm{w})} \qquad (11)$$

where $H_{\mathrm{pp}}^{(\mathrm{s})}$ (or $H_{\mathrm{ss}}^{(\mathrm{s})}$) is the solute internal potential energy when the precursor complex H_{pp} (or the successor complex H_{ss}) potential energy function is used, $H_{\mathrm{pp,i}}^{(\mathrm{s-w})}$ (or $H_{\mathrm{ss,i}}^{(\mathrm{s-w})}$) is the interaction energy between the solute molecule and the i water molecule when the precursor complex H_{pp} (or the successor complex H_{ss}) potential energy function is used, and finally, $H_{\mathrm{pp,ij}}^{(\mathrm{w})}$ (or $H_{\mathrm{ss,ij}}^{(\mathrm{w})}$) is the interaction energy between the i water molecule and the j water molecule when the precursor complex H_{pp} (or the successor complex H_{ss}) potential energy function is used.

Then, according the above definition of the reaction coordinate, we have

$$\Delta E = (H_{\mathrm{ss}}^{(\mathrm{s})} - H_{\mathrm{pp}}^{(\mathrm{s})}) + \sum_{\mathrm{i}} (H_{\mathrm{ss,i}}^{(\mathrm{s-w})} - H_{\mathrm{pp,i}}^{(\mathrm{s-w})}) = \Delta E^{(\mathrm{s})} + \Delta E^{(\mathrm{s-w})} \qquad (12)$$

where we have used

$$\sum_{\mathrm{i}}\sum_{\mathrm{j>i}} (H_{\mathrm{ss,ij}}^{(\mathrm{w})} - H_{\mathrm{pp,ij}}^{(\mathrm{w})}) = 0 \qquad (13)$$

That is, ΔE arises from the sum of many highly anharmonic random variables (note that there is a lot of solvent molecules). If the random variable $(H_{\mathrm{ss}}^{(\mathrm{s})} - H_{\mathrm{pp}}^{(\mathrm{s})})$ has not a too much large relative contribution (it is null for outersphere electron transfer reactions), the central limit theorem applies and the reaction coordinate ΔE tends to follow a normal distribution. In this case, the free energy curves would be quadratic and the Marcus' relationship would hold. For the sake of example, in Table 8 the mean values of the random variables $(H_{\mathrm{ss}}^{(\mathrm{s})} - H_{\mathrm{pp}}^{(\mathrm{s})})$ and $(H_{\mathrm{ss,i}}^{(\mathrm{s-w})} - H_{\mathrm{pp,i}}^{(\mathrm{s-w})})$ for the FHDE, FMDE, and FLDE simulations when the mapping potential H_{m} associated to $\lambda_{\mathrm{m}} = 0$ (reactants) or $\lambda_{\mathrm{m}} = 1$ (products) is used are presented. Indeed these data show that central limit theorem does not apply for the electrochemical reduction of methyl fluoride (FHDE simulation) because of the large size of the $(H_{\mathrm{ss}}^{(\mathrm{s})} - H_{\mathrm{pp}}^{(\mathrm{s})})$ relative contribution. Conversely, both FMDE and FLDE test simulations are much closer to the requirement of the theorem, in such a way that the roughly fulfillment of the Marcus' relationship that is exhibited in Table 7 can be justified.

Table 8. Mean Values (in kJ/mol) of the Random Variables $\mathrm{H}_{\mathrm{ss}}^{(\mathrm{s})}$–$\mathrm{H}_{\mathrm{pp}}^{(\mathrm{s})}$ and $\mathrm{H}_{\mathrm{ss,i}}^{(\mathrm{s-w})}$–$\mathrm{H}_{\mathrm{pp,i}}^{(\mathrm{s-w})}$ for the FHDE, FMDE, and FLDE Simulations When the Mapping Potential H_m Associated to $\lambda_m = 0$ (Reactants) or $\lambda_m = 1$ (Products) Is Used

	$\lambda_m = 0$		$\lambda_m = 1$	
simulation	$\mathrm{H}_{\mathrm{ss}}^{(\mathrm{s})}$–$\mathrm{H}_{\mathrm{pp}}^{(\mathrm{s})}$	$\mathrm{H}_{\mathrm{ss},i}^{(\mathrm{s-w})}$–$\mathrm{H}_{\mathrm{pp,i}}^{(\mathrm{s-w})}$	$\mathrm{H}_{\mathrm{ss}}^{(\mathrm{s})}$–$\mathrm{H}_{\mathrm{pp}}^{(\mathrm{s})}$	$\mathrm{H}_{\mathrm{ss},i}^{(\mathrm{s-w})}$–$\mathrm{H}_{\mathrm{pp},i}^{(\mathrm{s-w})}$
CH_3F(FHDE)	362.7	0.3	–1010.6	–5.1
CH_3F(FMDE)	67.6	0.2	–83.7	–5.0
CH_3F(FLDE)	28.0	0.2	–41.7	–5.1

Conclusions

In the present work we have performed microscopical Monte Carlo simulations of the electrochemical reductions of methyl fluoride and methyl chloride in water to give methyl radical and the corresponding halide anion. These are intented to be realistic models of a dissociative electron transfer reaction, a special case of an innersphere electron transfer process. Assuming a classical frame, the diabatic free energy curves corresponding to the precursor and successor complexes, in function of the reaction coordinate ΔE defined as the difference between the diabatic energy hypersurfaces for each configuration of the system, have been built up.

The results of the Monte Carlo simulations suggest that, unlike the outersphere electron transfer reactions, the linear response approximation cannot be applied straightforwardly to the dissociative electron transfer reactions in solution, its validity depending on the features of the solute internal potential energy. Despite the highly anharmonic character of the solute–solvent interactions, the central limit theorem justifies why the outersphere electron transfer reactions fulfills the Marcus' relationship. As for the dissociative electron transfer reactions, where a chemical bond is broken, several cases can be distinguished. If, for hazard, the gas phase diabatic pair potentials can be described by a Morse curve and its repulsive part, the Marcus' relationship holds both in gas phase and in solution. Normally, this will not be the case. Then, if the chemical bond to be broken is strong (this will imply a high dissociation energy) an important deviation of the Marcus' relationship, due to the large size of the solute relative contribution to the reaction coordinate ΔE, is suggested by our calculations. Conversely, if the chemical bond that undergoes the cleavage is weak enough to cause solute relative contributions to ΔE to be more or less equivalent to the solute–solvent contributions, the central limit theorem leads again to the Marcus' relationship. Evidently, many intermediate situations exist. So, our Monte Carlo simulations suggest that the direct extension to dissociative electron transfer reactions in solution of this very useful equation originally developed by Marcus to describe outersphere electron transfer reactions should be done with caution. On the other hand, further computational study of other innersphere electron transfer reactions would be desirable. In this sense, methyl cation transfer reactions in S_N2 processes (for which a lot of experimental results exists[56,57]) are particularly interesting.

Acknowledgment. Financial support from DGICYT ("Ministerio de Educación y Ciencia" of Spain) trough project No. PB92-0613 is gratefully acknowledged.

---

(55) Marcus, R. A. *Angew. Chem., Int. Ed. Engl.* **1993**, *32*, 1111.
(56) Albery, W. J.; Kreevoy, M. M. *Adv. Phys. Org. Chem.* **1978**, *16*, 87.
(57) Albery, W. J. *Annu. Rev. Phys. Chem.* **1980**, *31*, 227.